INSTITUTE OF PHYSICS PUBLISHING SEMICONDUCTOR SCIENCE AND TECHNOLOGY

Semicond. Sci. Technol. **22** (2007) 222–228 doi:10.1088/0268-1242/22/3/009

Electron transport and optical properties of shallow GaAs/InGaAs/GaAs quantum wells with a thin central AlAs barrier

V A Kulbachinskii[1], I S Vasil'evskii[1,3], R A Lunin[1], G Galistu[2], A de Visser[2], G B Galiev[3], S S Shirokov[3] and V G Mokerov[3]

[1] Low Temperature Physics Department, Moscow State University, 119992, GSP-2, Moscow, Russia
[2] Van der Waals-Zeeman Institute, University of Amsterdam, Valckenierstraat 65, 1018 XE Amsterdam, The Netherlands
[3] Institute of UHF Semiconductor Electronics, 117105, Moscow, Russia

E-mail: kulb@mig.phys.msu.ru

Received 25 June 2006, in final form 23 November 2006
Published 19 January 2007
Online at stacks.iop.org/SST/22/222

Abstract
Shallow GaAs/InGaAs/GaAs quantum well structures with and without a three-monolayer thick AlAs central barrier have been investigated for different well widths and Si doping levels. The transport parameters are determined by resistivity measurements in the temperature range 4–300 K and magnetotransport in magnetic fields up to 12 T. The (subband) carrier concentrations and mobilities are extracted from the Hall data and Shubnikov–de Haas oscillations. We find that the transport parameters are strongly affected by the insertion of the AlAs central barrier. Photoluminescence spectra, measured at 77 K, show an increase of the transition energies upon insertion of the barrier. The transport and optical data are analysed with the help of self-consistent calculations of the subband structure and envelope wavefunctions. Insertion of the AlAs central barrier changes the spatial distribution of the electron wavefunctions and leads to the formation of hybrid states, i.e., states which extend over the InGaAs and the delta-doped layer quantum wells.

1. Introduction

In the past 15 years research into quantum well (QW) structures with thin barriers has attracted considerable interest. Optical studies on, e.g., GaAs QWs with thin AlAs or $Al_{1-x}Ga_xAs$ barrier layers incorporated in the well region demonstrated that the energy spectrum of the two-dimensional electrons could be tuned by changing either the barrier thickness or its height [1, 2]. Such a tuning might be utilized, for instance, in infrared photodetectors or lasers [3].

For practical use of quantum well structures high electron mobilities are desirable, and therefore it is of much interest to suppress electron–phonon scattering, which is dominant in modulation doped quantum well structures at temperatures above 100 K. It has been suggested that this might be accomplished by inserting a thin barrier which acts as a phonon wall. For instance, in transport experiments reported in [4] an increase in the electron mobility was observed when three AlAs barriers were inserted into a GaAs/AlAs multiple QW [4]. The reduction in scattering rate was attributed to the confinement of optical phonons [4], but in a theoretical paper [5] another explanation of the effect was suggested, namely a modulation of electron states. In several theoretical papers [6–9] it has been calculated that the introduction of thin AlAs barriers in rectangular QWs leads to suppression of intersubband scattering by optical phonons, which in turn enhances the electron mobility. Other theoretical work has argued against an observable enhancement of the mobility [10, 11]. Clearly, consensus is lacking.

Surprisingly, until today no systematic transport studies have been undertaken for the case of a simple structure with a single barrier incorporated in the QW. The majority of the experimental work is devoted to the investigation of optical properties and subband formation in complex structures,

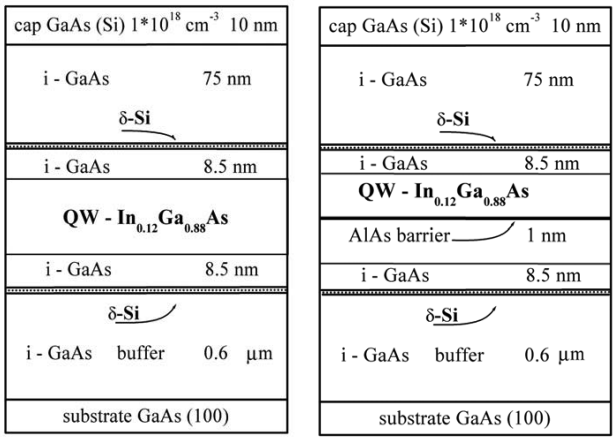

Figure 1. Schematic sample structure for the $In_{0.12}Ga_{0.88}As$ quantum wells: (*a*) without and (*b*) with an AlAs central barrier.

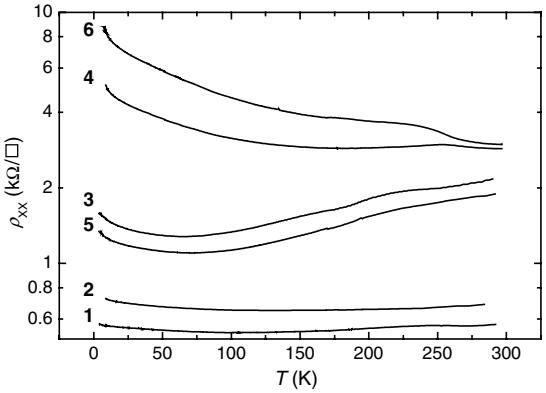

Figure 2. Temperature variation of the sheet resistance for the $In_{0.12}Ga_{0.88}As$ quantum wells with (2, 4, 6) and without (1, 3, 5) the AlAs central barrier.

e.g., heavily doped pseudomorphic high electron mobility transistors [12]. In this work we focus on electron transport properties of shallow InGaAs QW structures with a thin AlAs barrier incorporated in the centre of the QW. We investigate how the transport parameters depend on the doping level and QW width. The transport data reveal that in our structures the electron mobility decreases rather than increases upon insertion of the barrier. We demonstrate that this is due to a strong reconstruction of the electron states and the formation of 'hybrid' wavefunctions, i.e., a delocalization of the central wavefunction into the δ dopant layers. Concurrently, the dominant scattering mechanism changes from phonon to ionized impurity scattering.

2. Samples

Pseudomorphic $In_{0.12}Ga_{0.88}As$ quantum wells with and without an AlAs barrier were grown by molecular-beam epitaxy on semi-insulating (1 0 0) GaAs substrates. The structures are schematically shown in figure 1. The QW samples consist of the following layers: a GaAs buffer layer 0.6 μm thick, a Si δ-doping layer, a GaAs spacer layer 8.5 nm thick, the $In_{0.12}Ga_{0.88}As$ quantum well with well widths L_{QW} of 8 or 12 nm, a GaAs spacer layer 8.5 nm thick, an upper Si δ-doping layer, and an i-GaAs layer 75 nm thick. The latter was grown in order to eliminate surface potential effects. The structures were covered with a cap layer of Si-doped GaAs 10 nm thick. The substrate temperature was 510 °C for the pseudomorphic QW and 590 °C for the other layers. Samples were prepared with δ-doping layers with Si concentrations of 3.2×10^{12} cm^{-2} (heavily doped, samples 1 and 2) and $\sim 1 \times 10^{12}$ cm^{-2} (moderately doped, samples 3–6). Samples without (1, 3, 5) and with a barrier (2, 4, 6) were prepared. The barrier consists of three monolayers of AlAs grown in the centre of the QW. The growth was interrupted for 30 s before and after depositing the QW and barrier layers. Sample pairs (1, 2), (3, 4) and (5, 6) were prepared within the same growth cycle and differ by the barrier layer only.

Two remarks as regards our sample design are in place. Firstly, the pseudomorphic growth leads to restrictions as regards the structure design. Since the lattice parameters of GaAs and $In_yGa_{1-y}As$ are different, the thickness of the $In_yGa_{1-y}As$ layer may not exceed ~17 nm for $y \sim 0.15$ when a high quality crystal structure is desired. Consequently, the bandgap and the conduction band offset are about two times smaller than for conventional $Al_{0.2}Ga_{0.8}As$/GaAs heterostructures [13]. Secondly, in this work we focus on transport properties and, therefore, dopant layers form an indispensable ingredient of the semiconductor structure. Ionized impurity scattering in these layers is inherent to the sample design. One cannot move the δ-delta-layers away from the QW, because this would lead to a reduction of the transition efficiency of electrons from the ionized donors to the QW. This implies that the spacer layer cannot be too thick. A direct comparison of our results with those obtained by optical techniques on samples without dopant layers is therefore not possible.

The structural and electro-physical characterization of the samples has been reported in [14]. In order to carry out transport measurements all samples were prepared in Hall bar geometry by conventional lithography and wet etching. In order to attach current and voltage leads, AuGe/Ni/Au ohmic contact pads were made on the samples.

3. Transport properties

The temperature dependence of the sheet resistance measured for $T = 4.2$–300 K is shown in figure 2 for all samples. For the heavily doped samples 1 and 2 the resistance attains lower values and has a weaker temperature variation than for the moderately doped samples (3–6). The single QW samples 3 and 5 show metallic behaviour: i.e., the resistance decreases approximately linearly with decreasing temperature down to ~70 K, below which the resistance increases weakly. The temperature and magnetic field variation of the resistance below 70 K has been studied in detail and can be attributed to weak localization effects [15].

The insertion of the barrier has a pronounced effect on the sheet resistance, notably in the moderately doped samples, although the barrier is quite thin. In samples 4 and 6 the value of the resistance at $T = 4.2$ K increases by a factor 3

Table 1. Structural and transport parameters (at $T = 300$ K, 77 K and 4.2 K) of the InGaAs QW samples.

			$T = 300$ K		$T = 77$ K		$T = 4.2$ K	
Sample no.	L_{QW} (nm)	N_d (Si) (10^{12} cm^{-2})	n_H (10^{12} cm^{-2})	μ_H (cm^2 V^{-1} s^{-1})	n_H (10^{12} cm^{-2})	μ_H (cm^2 V^{-1} s^{-1})	n_H (10^{12} cm^{-2})	μ_H (cm^2 V^{-1} s^{-1})
1	12	3.2	2.72	3830	3.0	4 700	2.86	3 800
2	12+ b*	3.2	2.6	3150	2.33	5 420	2.61	3 300
3	12	1.04	0.54	5740	0.79	18 500	0.52	10 000
4	12+ b*	1.04	0.42	4810	0.78	5 300	0.57	2 070
5	8	1.1	0.53	5910	0.76	18 700	0.59	7 980
6	8 + b*	1.1	0.50	4000	0.87	3 570	0.47	1 520

* +b indicates samples with inserted central AlAs barrier (1 nm).

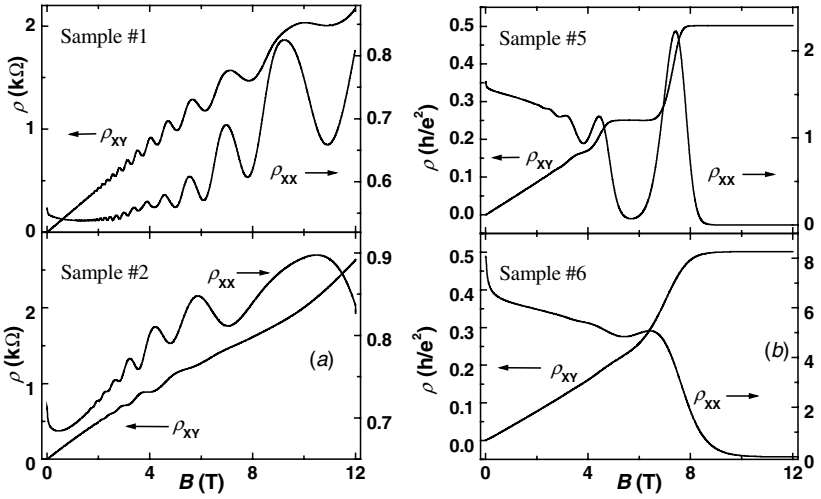

Figure 3. Longitudinal ρ_{xx} and transverse ρ_{xy} resistivity measured at $T = 0.25$ K for (*a*) samples 1 and 2 and (*b*) for samples 5 and 6.

and 7 compared to samples 3 and 5, respectively. The large difference in resistance due to insertion of the barrier decreases when the temperature increases. The resistance values of the single QW sample 5 are smaller than those of sample 3, although the well width is smaller ($L_{QW} = 8$ nm compared to 12 nm). This is due to the slightly larger carrier concentration in sample 5 (∼5%) as was determined by the low-temperature Hall data (see below).

Electron Hall densities n_H and Hall mobilities μ_H were determined at temperatures of 4.2, 77 and 300 K for all samples. An overview of the results is presented in table 1. For the heavily doped samples 1 and 2 the Hall density amounts to 2.6–2.7 × 10^{12} cm^{-2} and is roughly temperature independent (to within ∼10%). Also the mobility is quite low, which indicates that ionized impurity scattering is dominant. For the moderately doped single QWs (samples 3 and 5) the temperature variation of n_H and μ_H is consistent with the metallic behaviour observed in the resistance. The overall increase of the mobility with decreasing temperature is attributed to the reduction in phonon scattering rate. However, in the samples with a barrier, 4 and 6, the Hall mobility on the whole decreases with decreasing temperature. Interestingly, at low temperatures (4.2 K and 77 K) the insertion of the barrier leads to a strong reduction of mobility by a factor 3–5, although the Hall density is roughly constant or even shows an increase (<20%).

4. Shubnikov–de Haas oscillations and quantum Hall effect

The longitudinal R_{xx} and Hall resistance R_{xy} were measured for all samples in magnetic fields B up to 12 T in the temperature range 0.25–4.2 K. Typical results obtained at $T = 0.25$ K are shown in figure 3 for samples 1, 2, 5 and 6. The overall behaviour (non-oscillatory component) of the high-field magnetoresistance for the heavily and moderately doped samples is quite different: while for samples 1 and 2 the magnetoresistance has positive quadratic field dependence, for samples 3–6 only a (initially sharp) negative magnetoresistance is observed, which is indicative of weak localization in low-density two-dimensional semiconductor structures. Superposed on the monotonous component, the longitudinal resistance shows pronounced Shubnikov–de Haas (SdH) oscillations. In figure 4 we present the fast Fourier transforms of the $R_{xx}(1/B)$ dependences of the SdH signals, where we have scaled the frequency axis to yield the two-dimensional electron densities. For samples 1–5 one main frequency peak is found, which indicates the presence of at least one occupied high-mobility subband. For sample 2 a shoulder is visible in the Fourier transform, which indicates the occupation of a second subband. For sample 6 no clear frequency can be detected in the FFT, which is due to the low mobility (see table 1) and the long oscillation period which

Table 2. Transport parameters of the InGaAs QW samples 1–6. n_H is the Hall and n_{SdH} the Shubnikov–de Haas electron concentration measured at $T = 4.2$ K, μ_{SdH} is the quantum mobility determined from the SdH effect, n_i is the calculated subband concentration and μ_{qi} and μ_{ti} the calculated quantum and transport mobility, respectively, for subband i, due to ionized impurity scattering.

Sample no.	L_{QW} (nm)	Barrier AlAs (3 ML)	n_{SdH}	n_i (i) (10^{12} cm^{-2})	n_H	μ_{SdH}	μ_{qi} (cm^2 V^{-1} s^{-1})	μ_{ti}
			1.35	1.30 (0)		2 700	7 780	15 800
1	12	–		0.83 (1)	2.86		640	2 870
				0.61 (2)			470	2 160
2	12	+	–	1.05 (0)			880	3 150
			–	0.97 (1)	2.61		890	2 330
			0.66	0.65 (2)		1 660	2 090	4 600
			0.58	0.52 (3)			940	2 500
3	8	–	0.49	0.51 (0)	0.52	1 400	3 210	33 700
4	8	+	0.44	0.44 (0)	0.57	920	2 770	6 470
				0.1 (1)				
5	8	–	0.55	0.48 (0)	0.59	1 430	2 850	28 800
6	8	+	–	0.43 (0)	0.47	–	1 650	4 000
				0.13 (1)				

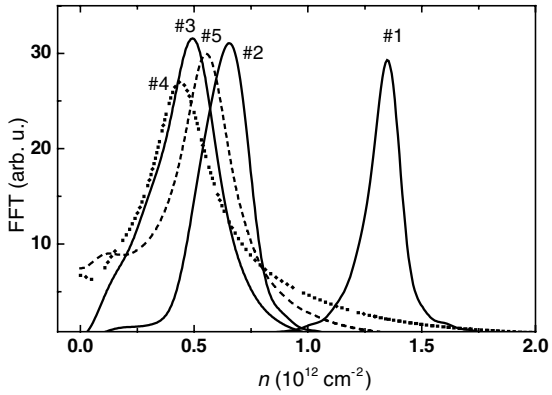

Figure 4. Fast Fourier spectra of the Shubnikov–de Haas data observed for samples 1–5 at $T = 0.25$ K. Note that the horizontal axis yields the SdH electron density.

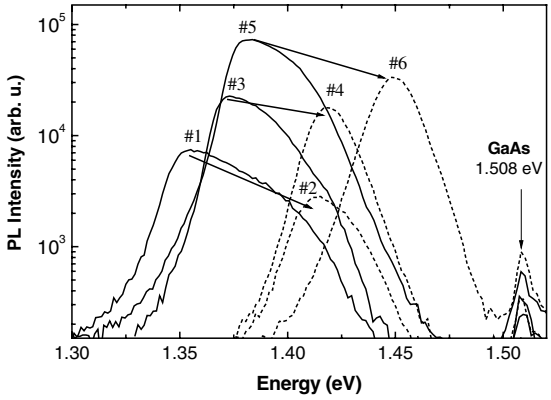

Figure 5. Photoluminescence spectra measured at 77 K for the $In_{0.12}Ga_{0.88}As$ quantum wells with (2, 4, 6) and without (1, 3, 5) the AlAs central barrier.

extends into the quantum Hall regime. The resulting values for the SdH density, n_{SdH}, are collected in table 2, together with the quantum mobilities, determined from the envelope of the SdH oscillations [16]. In the heavily doped samples n_{SdH} decreases considerably, i.e. from 1.35×10^{12} cm^{-2} to $\sim 0.6 \times 10^{12}$ cm^{-2}, when the barrier is inserted. The SdH densities are much lower than the Hall density, indicating that several subbands with different electron mobilities are populated. For the moderately doped samples the SdH and Hall densities are all of the same order (the Hall densities being 10–20% higher), which indicates that transport is dominated by a high-mobility subband. Note that the barrier insertion weakly decreases the carrier concentration in the moderately doped samples.

The transverse resistance R_{xy} for samples 3–6 shows the quantum Hall effect (QHE). The QHE is most pronounced in the samples without barrier, because of the higher mobility. For samples 3 and 5 clear integer plateaus are observed at $T = 0.25$ K for non-spin split Landau levels with filling factors $\nu = 4$ and $\nu = 2$ (see figure 3(*b*)). At the integer filling factors $R_{xx} = 0$, which demonstrates the absence of parallel conduction. In samples 1 and 2 parallel conduction due to the population of several subbands hampers the observation of the QHE.

5. Photoluminescence

The photoluminescence (PL) spectra of all samples have been measure at $T = 77$ K. The results are reported in figure 5. All PL spectra of the $In_{0.12}Ga_{0.88}As$ quantum wells exhibit a pronounced maximum in the energy range 1.35–1.47 eV, which is somewhat below the transition in bulk GaAs at 1.508 eV. For the single QWs (1, 3 and 5) the peaks are relatively broad and the PL intensity rise differs for the different sample, indicating the presence of several transition energies. For samples with a barrier (2, 4 and 6), the PL peaks are less broad, which indicates that the electron levels are more closely spaced. A most important observation is that incorporating the barrier leads to a significant upward shift of the spectra of the order of 0.06 eV, without a substantial decrease of PL intensity. We also note that for the single QW samples 1 and 3, which have the same well width $L_{QW} = 12$ nm but different doping levels, the transition energies differ slightly (by 0.02 eV). However, upon insertion of the barrier (2 and 4) this energy difference disappears.

6. Subband structure and wavefunctions

The conduction band profile and the subband structure were calculated for all the structures by solving the Schrödinger and

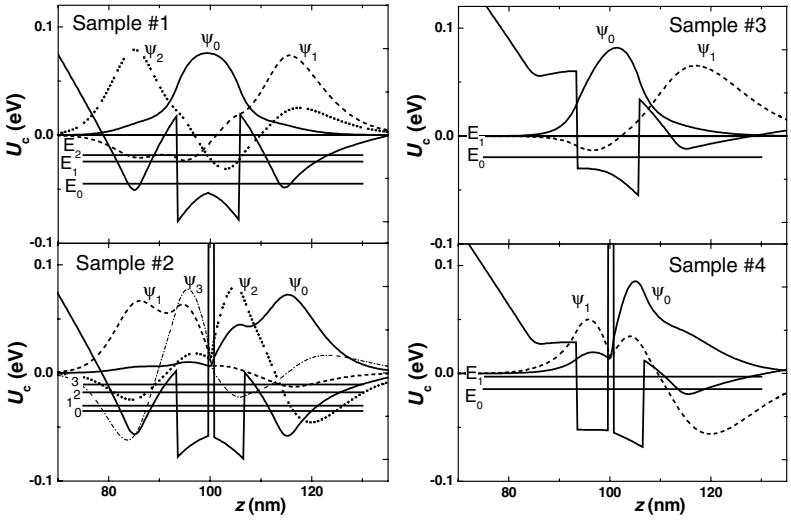

Figure 6. Calculated conduction band profiles, electron wavefunctions and subband energy levels for $In_{0.12}Ga_{0.88}As$ quantum wells with (2, 4) and without (1, 3) an AlAs central barrier.

Poisson equations self-consistently (see, e.g., [17]). In order to achieve adequate modelling of the δ-doped layer we used a finite distribution width of 5 nm, which is the characteristic width of the Si δ-layer in GaAs at the applied growth temperature [18]. The conduction band profiles for the heavily doped samples 1 and 2 and the moderately doped samples 3 and 4 are qualitatively different as shown in figure 6, where we have taken the Fermi level as zero energy reference. In the heavily doped samples the δ-doped layers form additional quantum wells almost symmetrically bordering the $In_{0.12}Ga_{0.88}As$ QW. In sample 1 the envelope wavefunction Ψ_0 of the ground state (energy E_0) is predominantly situated in the $In_{0.12}Ga_{0.88}As$ QW, but partially penetrates in the V-shaped δ-layer QWs. The wavefunctions Ψ_1 and Ψ_2 are mainly confined in the δ-layer QWs and result in two split subbands labelled E_1 and E_2. The calculated values of the subband electron concentration n_i (where i is the subband index) are reported in table 2. Insertion of the AlAs barrier (sample 2) results in a tunnel splitting of the central QW state into the wavefunctions Ψ_2 and Ψ_3 and an upward shift of the subband energies, now labelled E_2, E_3. Hence the central QW states are no longer the ground state of the whole system. The wavefunctions Ψ_2 and Ψ_3 are strongly reconstructed compared to Ψ_0 in sample 1, and rather form a hybrid state in the quantum well and δ-doped regions. The wavefunctions in the δ-doped wells (now Ψ_0 and Ψ_1) are less affected by the insertion of the barrier. The electron density increases in the region of the δ-doped wells and decreases in the QW region upon insertion of the barrier (see table 2). This is due to the relatively shallow central QW. Also band bending considerably affects the band structure. The formation of a hybrid state due to heavy doping has also been reported for InGaAs quantum wells [19].

In the moderately doped samples 3 and 5 the V-shaped δ-layer QWs are significantly weaker and band bending remains relatively small. Moreover, the conduction band profile is asymmetric: only one non-QW state Ψ_1 with energy E_1 forms below E_F in the δ-layer. This state is located in the lower δ-layer QW (i.e. at ~115 nm below the surface). The electron concentration n_1 in this subband is however negligible at low temperatures. The energy difference between the ground-state energy level E_0 and the level E_1 is high. Hence, the electrons in the ground-state subband of the single QW are largely confined in the QW (Ψ_0 for the sample 3, see figure 6). Just as in the case for the heavily doped samples, insertion of the barrier into the QW leads to a significant redistribution of the wavefunction towards the δ-doped region (Ψ_0 for sample 4). The energy level E_0 (and also E_F) shift up with respect to the QW bottom. E_1 increases due to Fermi level increase, and an associated electron concentration n_1 results from the calculations (see table 2).

7. Discussion

In the simple case of a single quantum well one expects that insertion of a central barrier leads to an increase of the energy levels and a decrease of the electron densities in the occupied subbands. The photoluminescence data are consistent with this idea and reveal an overall energy shift of ~0.06 eV. However, the transport measurements show that the situation is more complicated. In the moderately doped samples, e.g. sample 3, $n_{SdH} = 0.45 \times 10^{-12}$ cm^{-2}, which decreases only slightly upon insertion of the barrier (sample 4), i.e. less than ~10%. This is explained by the Fermi level shifting up with respect to the QW bottom, when the barrier is inserted. This causes the energy separation between the hole and electron bands to increase considerably, while the difference $E_F - E_i$ remains small (~2 meV). It is this latter energy difference which determines the carrier concentration. For the heavily doped samples (1 and 2) the transport measurements show that the difference $E_F - E_i$ indeed changes: for sample 1 n_{SdH} of the high-mobility subband associated with the central QW is 1.35×10^{-12} cm^{-2}, which decreases to $\sim 0.6 \times 10^{-12}$ cm^{-2} in sample 2.

The energy band structure calculations are most useful for clarification of the transport results as they reveal the strong influence of the V-shaped δ-layer QWs. The key feature is the delocalization of the central wavefunction into the δ-layer

region upon insertion of the barrier (hybrid state), which has its origin in the shallowness of the central QW and a relatively strong δ-doping level. To account for the unusual transport behaviour, the quantum μ_q and transport μ_t mobilities due to ionized impurities scattering have been calculated for the various subbands [20]. The results are collected in table 2.

Let us first consider the moderately doped samples, e.g., 3 and 4. The calculations show that while the barrier is added at the QW centre, the ground-state energy level E_0 shifts up with respect to the QW bottom (+22 meV), so its wavefunction Ψ_0 has now noticeable amplitude in the lower δ-layer (i.e. at 115 nm) QW. The decrease of the Hall mobility at all temperatures is naturally explained by the additional scattering contribution due to ionized impurities in the δ-layer regions when the hybrid state is formed. As follows from the data in table 2, the calculated transport mobility μ_t is high in the single QW samples 3 and 5, and much smaller in the QW samples 4 and 6 with a barrier. This confirms that in the latter samples ionized impurity scattering dominates. The decrease of the mobility is most pronounced in sample 6, i.e the sample with small $L_{QW} = 8$ nm, because the wavefunction Ψ_0 has the strongest amplitude in the δ-layer region.

In the heavily doped samples comparison of the SdH and Hall concentrations at $T = 4.2$ K reveals that the QW subband is occupied by slightly less electrons ($n_{SdH} = 1.35 \times 10^{12}$ cm^{-2}, calculated value $n_i = 1.3 \times 10^{12}$) than the subbands in the δ-layer potential wells (with a total electron density $\sim$1.4–1.5 $\times$ 10^{12} cm^{-2}). The insertion of the barrier (sample 2) effectively shifts the QW subband upwards (from E_0 to E_2 *and* E_3, i.e. an energy shift $\Delta E \sim 20$ meV), while E_F is 'stabilized' by the high electron concentration in the δ-layer QWs. Thus the hybrid wavefunctions Ψ_2 and Ψ_3 are now the central QW states. The mobility calculations show that the highest value (see underlined values in table 2) is obtained for the third subband with wavefunction Ψ_2. The observed SdH oscillation in sample 2 is attributed to the lowest hybrid QW state Ψ_2 and is consistent with the calculated value n_2. The mobility in this subband is still high, because (i) $|\Psi_2|^2$ is small in the δ-layer area and (ii) the electrons in the δ-layer QWs effectively screen the ionized impurity potential.

We conclude that for our shallow GaAs/InGaAs/GaAs quantum wells the strong modification of the subband structure upon insertion of the thin AlAs barrier is the main reason for the change of the electron transport properties. The dominant scattering mechanism changes from phonon to ionized impurity scattering. These findings stress the need for more sophisticated models. Note that the models employing electron phonon scattering presented in [6–9, 21] assume ideal QWs, without detailed modelling of the subband structure. For example, in [21] electron concentrations up to $n = 10^{13}$ cm^{-2} in the QW were used. These values are much too high and cannot be achieved experimentally in AlGaAs/GaAs QW systems.

It is of importance to remark that the strong modification of the subband structure reported for our QWs is hardly observed in the AlGaAs/GaAs/AlGaAs system for the range of electron concentrations investigated. This is due to the nearly two times higher conduction band offsets compared to GaAs/InGaAs/GaAs QWs [13], so a stronger band bending and higher electron concentration are needed to observe the hybridization effects. Hybrid states have been reported as well in a photoluminescence study of GaAs/InGaAs/GaAs QWs [19]. However, in this work the influence of hybridization on the transport properties has not been considered.

8. Summary

The transport and optical properties of shallow GaAs/$In_{0.12}Ga_{0.88}As$/GaAs quantum wells with and without a three-monolayer thick central AlAs barrier have been investigated. Magnetotransport and photoluminescence measurements were performed on samples prepared with two different quantum well widths and different Si doping levels. The PL data show an overall shift of the spectra to higher transition energies ($\Delta E \sim 0.05$ eV), while the electron concentration extracted from the Hall data decreases only slightly. The mobility decreases upon insertion of the central barrier. Self-consistent calculations of the subband structure and envelope wavefunctions reveal a strong influence of the δ-doping regions on the conduction band profile: additional V-shaped quantum wells are formed in the δ-doping regions. Consequently, the central QW wavefunction extends into the δ-doping regions and forms a 'hybrid' wavefunction. The hybrid character becomes more pronounced when the central barrier is incorporated in the structures and accordingly the electron density displaces towards the δ-layers. This results in a change of the dominant scattering mechanism from phonon to ionized impurity scattering.

Acknowledgments

This work was supported by the Russian Foundation for Basic Research, grant 05-02-17029a, a program of RAS 'Quantum Nanostructures', and FOM (Dutch Foundation for Fundamental Research of Matter).

References

[1] Schmiedel T, McCombe B D, Petrou A, Dutta M and Newman P G 1992 *J. Appl. Phys.* **72** 4753
[2] Zhao Q X, Wongmanerod S, Willander M, Holtz P O, Selvig E and Fimland B O 2000 *Phys. Rev.* B **62** 10984
[3] Trzeciakowski W and McCombe B D 1989 *Appl. Phys. Lett.* **55** 891
[4] Zhu X T, Goronkin H, Maracas G N, Droopad R and Stroscio M 1992 *Appl. Phys. Lett.* **60** 2141
[5] Tsuchiya T and Ando T 1993 *Phys. Rev.* B **48** 4599
[6] Požela J, Jucene V and Požela K 1995 *Semicond. Sci. Technol.* **10** 1076
[7] Požela J, Namajunas A, Požela K and Juciene V 1997 *J. Appl. Phys.* **81** 1775
[8] Požela J, Namajunas A, Požela K and Juciene V 1999 *Physica* E **5** 108
[9] Wang X F, Da Cunha Lima I C and Lei X L 1998 *Phys. Rev.* B **58** 12609
[10] Bennet C R, Amato M A, Zakhleniuk N A, Ridley B K and Babiker M 1998 *J. Appl. Phys.* **83** 1499
[11] Wang X F, Da Cunha Lima I C, Troper A and Lei X L 1999 *J. Appl. Phys.* **85** 6598
[12] Bouzaïene L, Sfaxi L, Sghaeïr H, Maaref H, Cavanna A, Jouault B, Contreras S and Konczewicz L 2001 *Opt. Mater.* **17** 299
[13] Vurgaftman I, Meyer J R and Ram-Mohan L R 2001 *J. Appl. Phys.* **89** 5815

[14] Vasil'evskii I S, Kulbachinskii V A, Galiev G B, Imamov R M, Lomov A A and Prohorov D Yu 2005 *Proc. Int. Conf. on Micro- and Nanoelectronics (Moscow, Zvenigorod, Rússia)* ed E Velikhov and K Valiev pp 2–23
[15] Kulbachinskii V A *et al* 2007 unpublished work
[16] Skuras E *et al* 1991 *Semicond. Sci. Technol.* **6** 535
[17] Kulbachinskii V A, Lunin R A, Rogozin V A, Fedorov Yu V, Khabarov Yu V and De Visser A 2002 *Semicond. Sci. Technol.* **17** 947
[18] Leuther A, Forster A, Luth H, Holzbrecher H and Breuer U 1996 *Semicond. Sci. Technol.* **11** 766
Schubert E F, Tu C W, Kopf R F, Kuo J M and Lunardi L M 1989 *Appl. Phys. Lett.* **54** 2592
[19] Abbade M L F, Iikawa F, Brum J A, Tröster Th, Bernussi A A, Pereira R G and Borghs G 1996 *J. Appl. Phys.* **80** 1925
[20] Kulbachinskii V A, Lunin R A, Kytin V G, Bugaev A S and Senichkin A P 1996 *JETP* **83** 841
[21] Požela J, Požela K and Juciene V 2000 *Semiconductors* **34** 1011